www.ietdl.org

Published in IET Wireless Sensor Systems
Received on 2nd August 2012
Revised on 29th April 2013
Accepted on 7th May 2013
doi: 10.1049/iet-wss.2012.0094

ISSN 2043-6386

Generic correlation model for wireless sensor network applications

Rajeev K. Shakya, Yatindra N. Singh, Nishchal K. Verma

Department of Electrical Engineering, Indian Institute of Technology, Kanpur, Uttar Pradesh 208016, India
E-mail: rajeevs@iitk.ac.in

Abstract: In wireless sensor networks (WSNs) having a high density of sensor nodes, transmitted measurements are spatially correlated, often redundantly whenever an event of interest is detected. In this work, the authors propose a correlation model to enable energy-efficient methodologies that exploit the spatial correlation at the network and medium access control (MAC) layers. At the network layer, the authors first demonstrate how, through proper tuning of both the sensing range and correlation threshold, WSNs can be partitioned into disjoint correlated clusters without degrading the information reliability, thus enabling significant energy saving. On the other hand, as another contribution, the authors investigate the impacts of correlation between nodes on achieved distortion in the event estimation at the sink. The interactions among various parameters such as distortion constraints, spatial node density, node selection, sensing range and their impacts on the reconstruction performance are quantitatively studied. The authors demonstrate that the same level of distortion constraint can be achieved by selecting fewer nodes. The nodes can be still fewer if they are less spatially correlated. However, the MAC protocols which show distributive effect of this selection needs more study.

1 Introduction

The recent developments in low-cost, low-power sensor nodes, which are capable of sensing, computing and transmitting sensory data over a large geographical area by cooperatively monitoring physical or environmental conditions, for example, temperature, sound, vibration, pressure etc. have enabled many sensor network applications. WSNs usually comprise of a large number of sensor nodes deployed randomly in a highly dynamic and hostile environment. Since the sensing coverage (sensing range) and network connectivity (communication range) are usually constant in a random deployment, a high density of redundant nodes is used to maintain the desired level of coverage in order to achieve sufficient sensory data resolution. In addition, WSNs are usually event-driven systems, where several nodes try to transmit data when any event of interest happens. Thus, the collective efforts of these sensor nodes play an important role in reliable event detection [1]. Since the sensor nodes are densely deployed, transmissions of information from the nodes to the sink are spatially correlated. The redundant correlated data are observed because of the common sensing area between nodes. The degree of spatial correlation increases with the increase in common sensing area between nodes. Therefore every sensor node observing the event need not be active for sensing and communication. A significant amount of energy saving is possible by taking advantage of spatial correlation. This has motivated researchers to develop more energy-efficient communication protocols for sensor network applications taking advantage of correlation.

Correlation in WSNs has been discussed in [1] and its exploitation has been studied in [2–7, 8]. Sensor scheduling methods based on sensing coverage have also been proposed in the literature. Lot of research efforts have been devoted to coverage-based scheduling methods to reduce redundancy based on the sensing range of nodes [9, 10]. Recently, coverage and connectivity problems have been considered jointly in [11, 12]. Also, investigations to have efficient communication protocols on the basis of correlation have been done [3, 4, 7, 13]. Several methods have been proposed to allow a smaller number of sensing nodes to transmit their reports from the event area, so as to reduce the power expenditure and to avoid unnecessary contention among correlated nodes [2, 3, 14].

In this paper, a basic spatial correlation function has been proposed to model the correlation characteristics of the event information observed by multiple omni-directional sensor nodes. A mathematical analysis using the proposed correlation model is also presented. Furthermore using this model, a theoretical framework has been developed to estimate the event source and the reconstruction distortion at the sink. On the basis of correlation model, the node selection strategies for event notification are possible, which will lead to more energy efficiency.

One can also have a scenario when sensor nodes have variable sensing ranges. This paper shows that energy can be saved in the data transmission process when nodes change their sensing range according to their positions and neighbourhood. When omni-directional sensors are used, sensing range of sensor nodes can be optimised based on the common overlapping coverage area with its neighbours.

This avoids redundancy by reducing the correlation in reported data. The allowed maximum correlation in measured information, observed by the nodes, while detecting an event, is decided by the user applications in terms of reliability/fidelity. Thus, the required event reliability at the sink can be maintained by dynamic optimisation of sensing range, that is, sensing range of nodes can be decreased or increased depending on the high or low density of nodes, respectively, in its vicinity.

Section 2 briefly discusses a sensor deployment model and states the objective of this work. A novel spatial correlation function is introduced and discussed in Section 3. Few of the applications which use the proposed correlation model, with simulation results, are discussed in Sections 4 and 5. In addition, Section 5 also gives a comparative study with existing correlation models. Lastly, Section 6 presents the concluding remarks.

2 Sensor deployment and problem description

Consider a dense WSN, where a large number of sensor nodes are scattered in an area, where events are to be observed. All nodes have equal initial energy and similar capabilities (communication, processing and sensing of events). All sensor nodes follow the omni-directional sensing, in which each node can reconstruct every point in an r-radius disk area centred at its location. A sensor node can detect all events within such a disk, whereas no event outside the disk can be detected [15, 16]. Each node has variable sensing range for detecting the events and fixed transmission range for communication. The communication range is usually much larger than the sensing range. The sink node is assumed to be interested only in a collective report about the event from all the nodes and not in individual reports from each node.

In general, a high density of sensor nodes is required to provide full coverage of the area under observation. When the number of nodes is more than the minimum required number of nodes in the field, multiple nodes detect the same event simultaneously, resulting in the generation of the redundant reports about a detected event. As shown in Fig. 1, nodes A, B, C and D are shown with their respective sensing ranges, which are indicated by dashed circles. Here, the sensing area of node B is also fully covered by its neighbours A, C and D together. Therefore event information observed by the sensor node B will also be sensed by its neighbours. B is found to be a redundant node in this case as even if B is not there, the event reporting will happen. The high density of redundant nodes in a WSN permits higher data resolution, but at the expense of energy used in transmitting extra data to the sink. It is desirable to limit the number of reporting nodes to just achieve the desired resolution. Motivated by this, we formulate the problem statement as follows.

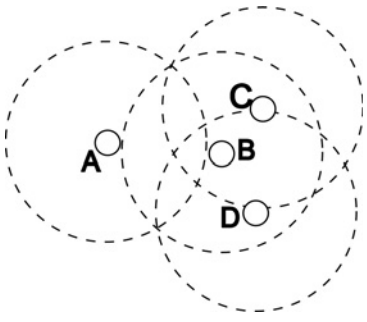

Fig. 1 *Coverage area of nodes, indicating that node B is redundant*

For a certain area of interest, suppose there is a set of N omni-directional sensor nodes that can detect an event within sensing range r. We denote them as $\mathcal{N} = \{n_1, n_2, n_3, \ldots\}$ with the spatial coordinates being denoted as $\{s_1, s_2, s_3, \ldots\}$. There exists correlation among these nodes which can be estimated based on their spatial coordinates. This spatial correlation can be exploited for the design of more energy-efficient communication protocols in WSN by avoiding transmissions from redundant nodes.

3 Correlation model

In this section, a correlation model between omni-directional sensor nodes have been presented. It should be noted that correlation between sensory data of two nodes is related to spatial correlation between them [1–4, 7, 13]. The spatial correlation can be estimated based on sensory coverage of nodes [17, 18]. The base station (i.e. the sink) needs to know the locations of nodes and sensing range r, to estimate the correlation. Thus, base station can estimate a more accurate sensed parameter by combining the received data while considering the estimated spatial correlation as the correlation between the received sensory data.

Assuming that all the received sensory data from reporting nodes is jointly Gaussian, the covariance between the two measured values from nodes n_i and n_j at location s_i and s_j, respectively, can be expressed by

$$\mathbb{C}ov\{s_i, s_j\} = \sigma_S^2 K_\vartheta\left(\|s_i - s_j\|\right) \tag{1}$$

Here, σ_S^2 is the variance of sample observation from sensor nodes and $\mathbb{C}ov(.)$ represents mathematical covariance. We assume σ_S^2 to be same for all the reporting nodes. $\|.\|$ denotes the Euclidean distance between nodes n_i and n_j. $K_\vartheta(.)$ denotes correlation function with $\vartheta = (\theta_1, \theta_2, \ldots, \theta_c)$ as the set of control parameters, which will be discussed later in this section.

3.1 Mathematical model design

Symbols and notations used in Fig. 2 are given in Table 1. If $d_{(i,j)} < 2r$, then $\mathcal{S}_i$, $\mathcal{S}_j$ will have an overlap. We can define the correlation as

$$\rho_{(i,j)} = K_\vartheta(d) = \frac{A_i^j + A_j^i}{A} \tag{2}$$

Here, $K_\vartheta(d)$ is the decreasing function with distance $d_{(i,j)}$, following the limiting value of 1 at $d = 0$ and of 0 for $d \geq 2r$. Areas A_i^j and A_j^i are same because of the symmetry as shown in Fig. 2

$$A_i^j = A_j^i = r^2 \cos^{-1}\left(\frac{d_{(i,j)}}{2r}\right) - \frac{L_{ij} d_{(i,j)}}{4} \tag{3}$$

Here, L_{ij} is the length of chord formed by intersection of two

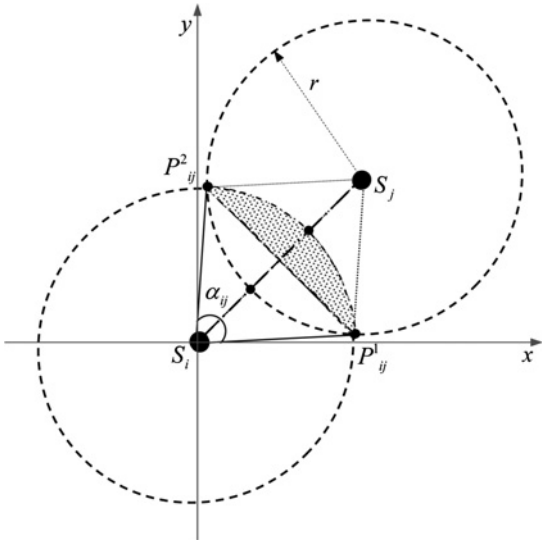

Fig. 2 *Spatial correlation model*

Table 1 Notations used in Fig. 2

Symbol	Description
$\mathcal{S}_i$	sensing region of node n_i of r-radius disk centred at itself
$\mathcal{S}_j$	sensing region of node n_j of r-radius disk centred at itself
A	area of the sensing region of a node
$d_{(i,\,j)}$	distance between nodes n_i and n_j located at s_i and s_j
$\left(P^1_{ij},\ P^2_{ij}\right)$	intersection points of two r-radius disk nodes
L_{ij}	length of common chord length which is equal to length of the line segment joining two intersection points P^1_{ij} and P^2_{ij}
A^j_i	area of region surrounded by arc denoted by $\overset{\frown}{P^1_{ij}P^2_{ij}}$ for S_i and chord denoted by $\overline{P^1_{ij}P^2_{ij}}$ as shown by the shaded area
A^i_j	area of region surrounded by arc denoted by $\overset{\frown}{P^1_{ij}P^2_{ij}}$ for S_j and chord denoted by $\overline{P^1_{ij}P^2_{ij}}$
$K_\vartheta(\|l\|.\|l\|)$	correlation matrix computed by a node with its neighbours

circular disks and is given by

$$L_{ij} = 2\sqrt{\left(r^2 - \frac{d^2(i,\,j)}{4}\right)}$$

From (2), we obtain

$$\rho_{(i,j)} = \frac{2\cos^{-1}\left(\left(d_{(i,j)}\right)/2r\right)}{\pi} - \frac{d_{(i,j)}}{\pi r^2}\sqrt{\left(r^2 - \frac{d^2_{(i,j)}}{4}\right)} \quad (4)$$

Let ϑ be a control parameter equal to $2r$. Then, (4) can be simplified as

$$\rho_{(i,j)} = \frac{2\cos^{-1}\left(d_{(i,j)}/\vartheta\right)}{\pi} - \frac{2d_{(i,j)}}{\pi\vartheta^2}\sqrt{\left(\vartheta^2 - d^2_{(i,j)}\right)} \quad (5)$$

We see that when $d_{(i,\,j)} = 2r$, the correlation model gives zero value. It means that there is no correlation between sensor nodes. For this reason, we introduce a control parameter ϑ equal to $2r$, as a variable to control the degree of correlation between nodes. The correlation model can be rewritten in a general form as (see (6))

It can be seen from (6) that when correlation function $K_\vartheta(d)$ is 0, it means that there is no correlation between the sensor nodes n_i and n_j, located at a distance $d_{(i,\,j)}$ from each other. If the correlation function $K_\vartheta(.)$ is equal to 1, the sensor nodes are perfectly correlated. The control parameter, ϑ is twice the sensing range of nodes. For the set of sensing ranges being $r = (2,\ 4.5,\ 6,\ 7.5,\ 9,\ 10)$, the set of control parameters, ϑ are $(\theta_1 = 4,\ \theta_2 = 9,\ \theta_3 = 12,\ \theta_4 = 15,\ \theta_5 = 18,\ \theta_6 = 20)$, respectively.

3.2 Correlation function, $K_\vartheta(\cdot)$ – examples

In this subsection, we simulate 200 randomly distributed nodes in a $150 \times 150\ \text{m}^2$ area as shown in Figs. 3*a* and *b*, 150 nodes in a $150 \times 150\ \text{m}^2$ area as shown in Fig. 3*c* and 30 nodes in a $50 \times 50\ \text{m}^2$ area as shown in Fig. 3*d*. The correlation between nodes is studied with variations in the control parameter ϑ. If the value of $\rho_{(i,\,j)}$ between two nodes is greater than zero, then they are shown using a connected solid line. In Figs. 3*a* and *b*, when a node-pair does not show any correlation [$\rho_{(i,\,j)}$ is equal to zero] both the nodes are out of sensing range from each other and there is no connecting line between them. Fig 3*a* with a distribution of 200 nodes with $\theta_1 = 9$ m (or $r = 4.5$ m) shows only a few connected lines indicating that very few nodes are correlated with their neighbours. Given the same location of the nodes, if we change the sensing range to $\theta_2 = 12$ m (Fig. 3*b*), more connected lines appear. This indicates that more nodes are now correlated with their neighbouring nodes. When node density changes for a given fixed sensing range (i.e. θ_1), more neighbouring nodes are correlated (Figs. 3*b* and *c*). Fig. 3*d* shows the correlation values on the lines connecting any two nodes.

3.3 Discussion

In sensor network applications, as long as the area of interest is specified, the correlation characteristics of the sensory observations of nodes can be obtained as described in the previous section. The proposed model is a generic correlation model that can be applied to all sensor network applications. Omni-directional sensing model is the traditionally used sensing model for WSNs. Generally, sensor nodes can be equipped with temperature, humidity, magnetic field sensors etc. as required. These sensors can operate in a range of 360° around the node. Hence, our correlation model is valid for most of the WSNs [16].

$$\rho_{(i,j)} = K_\vartheta(d) = \begin{cases} \dfrac{2\cos^{-1}\left(\left(d_{(i,j)}\right)/\vartheta\right)}{\pi} - \dfrac{2d_{(i,j)}}{\pi\vartheta^2}\sqrt{\left(\vartheta^2 - d^2_{(i,j)}\right)}, & \text{if} \quad 0 \le d_{(i,j)} < \vartheta^2 \\ 0, & \text{if} \quad d_{(i,j)} \ge \vartheta^2 \end{cases} \quad (6)$$

doi: 10.1049/iet-wss.2012.0094

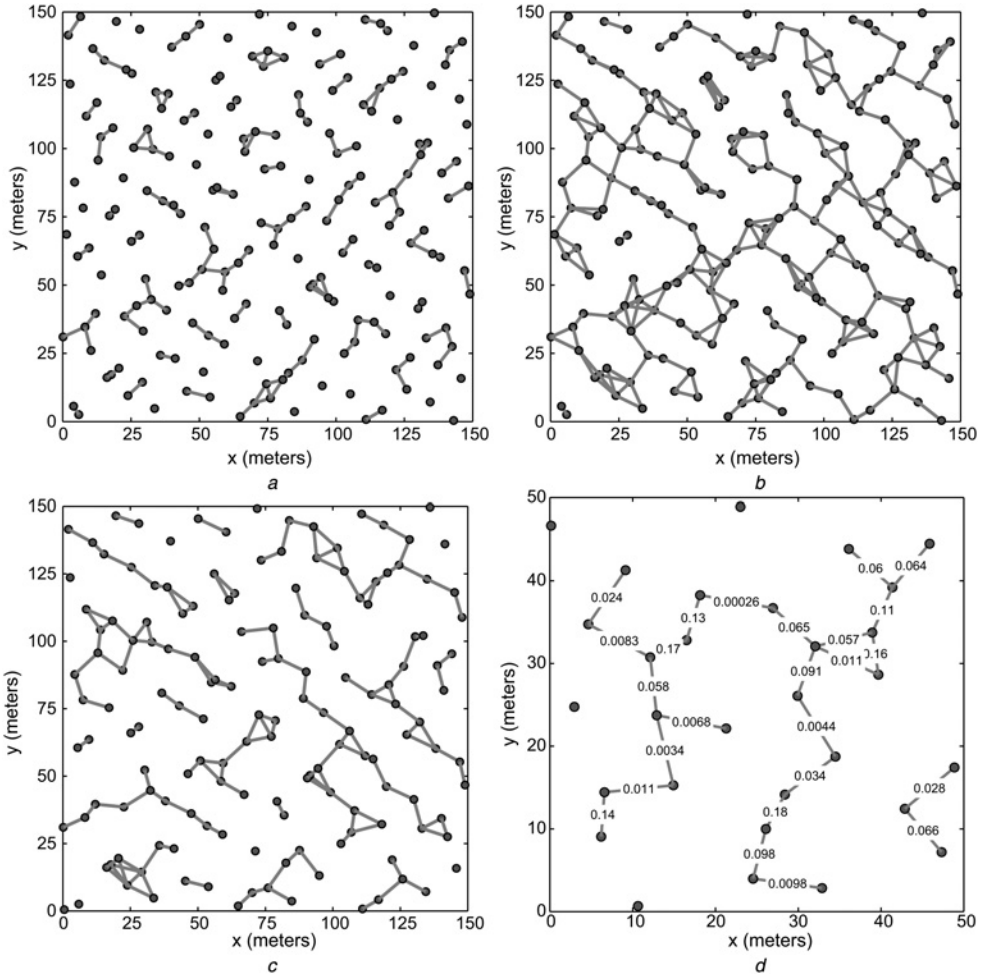

Fig. 3 *Random distribution for 200 nodes*

a θ_2 = 9 m
b θ_2 = 12 m
c 150 nodes with θ_2 = 12 m
d 30 nodes with θ_1 = 9 m

In addition, the proposed correlation model can provide the guidelines for designing energy-efficient communication protocols for most of the WSNs. Whole network can be partitioned into correlated clusters using the presented model. To gain more insight into energy-efficient operation at network layer using proposed correlation model, an analysis has been presented in Section 4.

In order to design an energy-efficient MAC protocols, researchers [2, 3] have used correlation functions [19] to determine the relationship between the spread of sensor nodes and event estimation reliability. In [2, 3], it has been argued that achieved distortion strongly depends on the following two factors: (i) the positive effect of the 'correlation coefficient', $\rho_{(i,j)}$, between each pair of representative nodes n_i and n_j as the distortion decreases with increase in the distance between nodes and (ii) the negative effect of the 'correlation coefficient', $\rho_{(s,i)}$, between the event source S and representative node n_i sending the event information as the distortion increases with increase in the distance between event source and the node. In this case, the location of the event source S is the necessary requirement to estimate the $\rho_{(s,i)}$. Unlike existing models [2, 3] that consider the exact location of S, a framework has been developed in Section 5 using the proposed model. Using this framework, the event information can be reconstructed at the sink without source location of any occurring event. Thus, our design presented in Section 5 will be more suitable for real network scenarios for given sensing range, location of nodes and distance between them. A comparative study on event distortion has also been carried out using our proposed correlation model and the earlier correlation models [2, 3].

4 Exploiting spatial correlation at the network layer

Using the proposed model, we introduce the possible approaches that takes the advantage of spatial correlation for energy-efficient communication protocols. This model has been used at the networking layer in this section, and the MAC layer in the next section. Both approaches take the advantage of spatial correlation for energy conservation in WSNs.

4.1 Partition of WSN in correlated clusters

Larger the overlap area between nodes, stronger will be the spatial correlation between them. We can define a correlation threshold ξ ($0 < \xi \leq 1$). If $K_\vartheta(d) \geq \xi$, then node

n_i and node n_j are strongly correlated. If $K_\vartheta(d) < \xi$, then node n_i and node n_j are weakly correlated. The correlation depends on sensing radius r (i.e. $\vartheta/2$) and node density in the event area. For highly correlated n_i and n_j

$$K_\vartheta\left\{\|s_i - s_j\|\right\} \geq \xi \tag{7}$$

Using (6), we obtain

$$\frac{2\cos^{-1}\left(d_{(i,j)}/\vartheta\right)}{\pi} - \frac{2d_{(i,j)}}{\pi\vartheta^2}\sqrt{(\vartheta^2 - d_{(i,j)}^2)} \geq \xi \tag{8}$$

When correlation is ξ, $d_{(i,\,j)} = R_{\text{corr}}$, that is

$$\xi = \frac{2\cos^{-1}\left(R_{\text{corr}}/\vartheta\right)}{\pi} - \frac{2R_{\text{corr}}}{\pi\vartheta^2}\sqrt{\left(\vartheta^2 - R_{\text{corr}}^2\right)} \tag{9}$$

For $d_{(i,\,j)} < R_{\text{corr}}$, $K_\vartheta\{\|s_i - s_j\|\} \geq \xi$.

If any node n_k is lying within R_{corr} from node n_i, it is within a strongly correlated distance from n_i. Otherwise, the correlation is weak. The value of ξ can be determined according to the requirements of the application, that is, data resolution with desired reliability at the sink. A larger value of ξ implies stronger correlation. For the given parameters ϑ and ξ, a densely deployed WSN can be partitioned into disjoint clusters of size R_{corr}. The cluster identification is basically the clique-covering problem over correlation graph, which is NP-hard [20]. A correlation graph G can be created where each node is represented by vertex, and edge (u, v) is drawn if the value of $\rho_{(u,\,v)}$ between nodes u and v is greater than or equal to ξ. As long as the correlation threshold ξ and the correlation function $K_\vartheta(.)$ are given, the sets of correlated clusters are determined through a hierarchical clustering process. Details of this algorithm are presented in Appendix 1.

4.2 Correlation based energy-efficient data collection

According to the discussion in previous subsection, when a greedy correlated clustering algorithm is used, sets of correlated clusters are formed and all nodes in a cluster are considered highly correlated. The information is observed by multiple sensor nodes in the event area creating redundant reports. This can be eliminated by exploiting spatial correlation. Only a few nodes need to report their sensory data, and the remaining nodes can remain in a silent state to save energy. The best way to make the proposed correlation model work is to partition the entire event area into correlated, disjoint and equal-sized hexagons with radius R_{corr}.

By exploiting redundancy in sensor observations within correlated cluster, saving of energy is possible at the network layer. Since all nodes in a cluster can be treated equally and only a small fraction of nodes (or at least one node) are allowed to be active to serve as the representative (s) of the whole cluster. The remaining nodes in the cluster can be kept in the sleep state. Thus, network lifetime can be increased when nodes within a cluster share the workload.

Since all nodes in each correlated cluster most likely observe the same event information, it is desirable to schedule only one node at a time to pass on that information to the sink, in order to save energy within the cluster. Within each cluster, time division multiple access (TDMA) scheme can be implemented to assign different time slots to each node that will schedule the work sequentially in a cluster. A round-robin scheduling method can be adopted in the clusters [12]. For a cluster with k sensor nodes, the period T can be divided into k time slots. In every T time duration, every sensor node will work only for a (T/k) time period. Initially, the sensor nodes should be time synchronised, and then the sink node can randomly assign a working schedule to the sensor nodes for each cluster.

We simulated the correlation-based clustering using the proposed Algorithm 1 (Appendix 1) by placing 60 nodes with a sensing range of 20 m for different values of ξ. The results are shown in Fig. 4. It is clearly seen that the number of correlated clusters and the number of member nodes in a cluster depend on the value of the correlation threshold ξ. If ξ is smaller a larger number of nodes falls in a correlated cluster on an average. On the other hand, a larger value of ξ allows a lesser number of correlated nodes in a cluster. Similarly, for different values of ϑ with fixed

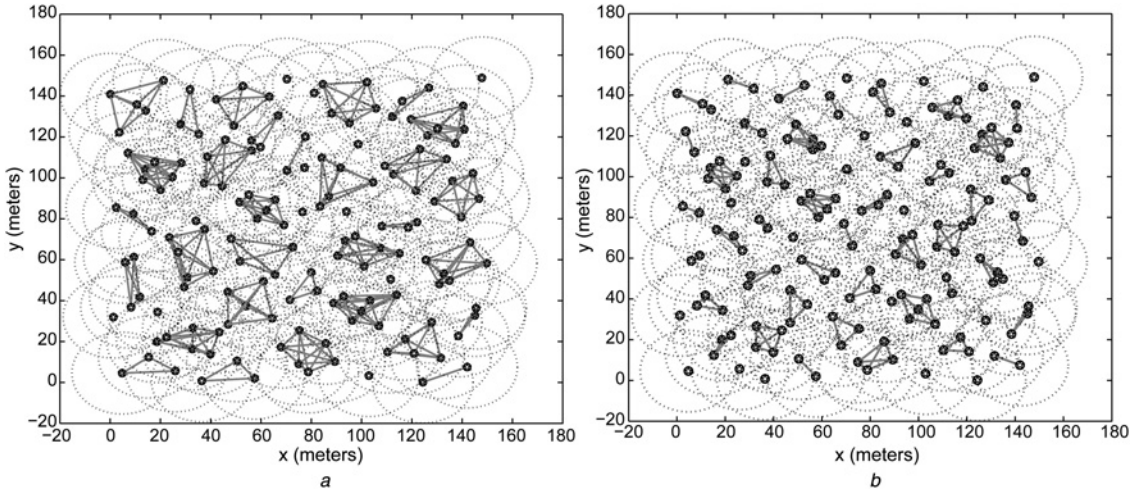

Fig. 4 *Correlation-based clustering results using algorithm 1 for 150 sensor nodes with $\theta_1 = 40$ m*

a $\xi = 0.25$
b $\xi = 0.5$

doi: 10.1049/iet-wss.2012.0094

Table 2 Results of R_{corr} for different values of ϑ and ξ

ϑ, m	ξ				
	0.2	0.4	0.5	0.6	0.8
9	5.78	4.11	3.51	2.3	1.25
12	8.03	5.5	4.7	3.05	1.7
15	10.04	6.23	5.87	3.86	2.16
18	12.07	8.23	7.05	4.67	2.59
21	14.0	9.6	8.23	5.44	3.02
24	16.13	11.07	9.39	6.22	3.46

node density, the sensor network is partitioned into different-sized correlated regions. Hence, the required information reliability/fidelity can be achieved through proper clustering by controlling parameters ϑ and ξ in data collection. Table 2 shows the results of R_{corr} for different values of ϑ and ξ.

The event area observed by the sensor nodes might change because of a change in environmental conditions. In this case, based on the reliability requirements, the sink node should decide whether the current clusters are valid or not. Then it should re-adjusts the clusters as quickly as possible by tuning the parameters ϑ and ξ and re-executing Algorithm 1. Thus, data reliability can be improved by re-partitioning of the whole network.

5 Exploiting the spatial correlation at MAC layer

Several MAC protocols have been proposed to take advantage of spatial correlation. Some of them have been analysed in [1–3, 14]. In this section, we first present a framework, using our correlation model to compute estimation error in terms of event distortion. Here, our objective is to choose the minimum number of nodes inside the event area such that the final achieved event distortion is within the tolerable distortion constraints. A comparative case study has also been presented with the existing models.

5.1 WSN model

Consider a WSN, where N sensor nodes are evenly distributed over a measurement field $\mathcal{D}(\mathcal{D} \subset \mathcal{R}^2)$. The event source S occurs inside the field $\mathcal{D}$ and is located in the centre of the event area. The nodes falling in the event area will have threshold exceeded (called reporting nodes) and thus send the sensory information to the sink. The WSN should be designed to minimise mean square error (MSE) distortion between event source S and its estimation $\hat{S}$ from the sensors' collective observations. The MSE distortion of the event is defined as a reliability measure required by the sensor applications. It is given as

$$D_E = \mathbb{E}\left[d_E(S, \hat{S})\right] \tag{10}$$

Here, $d_E(S, \hat{S})$ is the event MSE distortion measure and $\mathbb{E}(.)$ represents mathematical expectation. In this paper, we refer D_{max} as the maximum tolerable information distortion allowed in the sensor network as per the application requirement. The sink reconstructs an estimate of the event source by exploiting the spatial data correlation while ensuring given distortion constraint D_{max} (i.e. $D_E \leq D_{max}$).

A simple Gaussian sensor network is considered as Gaussian distribution usually having maximum entropy. We assume that an event can happen anywhere in the field, denoted by event source S. The event source S can be modelled as a random process $s(t, x, y)$ at a time t and spatial coordinate (x, y). We can approximately estimate the (x, y) as centroid of all the reporting nodes. The weighted average of the information sensed by all the reporting nodes will give the estimate $\hat{S}$. We also assume that N nodes sense the event and send the information to the sink. Let a node n_i observe the event S as S_i. Owing to noise and other imperfections, the sensed data will be X_i. The node n_i encodes X_i and transmits it to the sink through multi-hop transmission. The sink node decodes all the received X_i's to estimate the S_i's. The encoder and decoder are denoted by E and D, respectively, as shown in Fig. 5. The variance of event information X_i is assumed to be same as variance of event source S. After collecting the event information X_i from node n_i, the sink estimates values of event information using the best estimator.

As the sensor nodes send the event information only when it is above a threshold, the mean value of data received from the reporting nodes is expected to be above threshold. As Fig. 5 shows, once the event of interest happens, node n_i observes the signal X_i with noise, at time t. Since samples are temporally independent, we neglect the time index t

$$X_i = S_i + N_i; \quad i \in N \tag{11}$$

Here, measured information X_i is assumed to be jointly Gaussian random variable (JGRV) and N_i is zero-mean Gaussian noise with variance σ_N^2. Hence

$$\mathbb{E}[S_i] = m_i, \quad \mathbb{V}ar[S_i] = \sigma_S^2,$$
$$\mathbb{V}ar[N_i] = \sigma_N^2, \quad i = , 2, \ldots, N$$

and

$$\rho_{(i,j)} = K_\vartheta(d_{(i,j)}) = \frac{\mathbb{E}\left[\left(S_i - m_i\right)\left(S_j - m_j\right)\right]}{\sigma_S^2} \tag{12}$$

Here $\rho_{(i,j)}$ is the correlation coefficient between nodes n_i and n_j located at coordinates s_i and s_j. The $d_{(i,j)}$ is the distance between these nodes and $\mathbb{V}ar(.)$ represents mathematical variance. The function $K_\vartheta(.)$ can be determined using the correlation model discussed in the earlier section.

In the literature, 'Spherical, Power exponential, Rational quadratic and Matérn' [19] correlation models have also been proposed. For the case of sensor network with omni-directional sensor nodes, these conventional models do not consider the real network conditions, such as sensing range, location of nodes and distance between nodes etc. Our proposed model first needs the coordinates of node placements and sensing range. Although the earlier

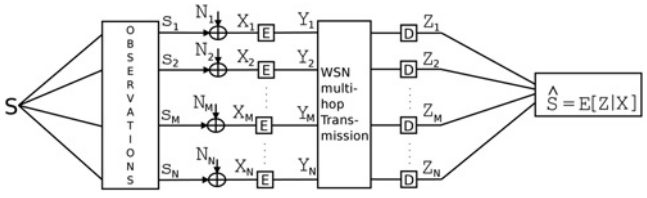

Fig. 5 *WSN model for event source S estimation*

proposed ones do not use these parameters. It should be noted that when node placement and sensing range are unknown, our model cannot be used. Therefore the correlation models must be chosen according to the properties of the physical phenomena and the sensed events' features. The events' features vary significantly for the energy-radiating physical phenomenon originating in the field. In this paper, we have considered those events which trigger all nodes within a radius of sensing range. They do not trigger nodes which are out of range irrespective of value of S.

Assuming S represents energy-radiating signal that propagates. The signal strength of event source S decays with distance and it follows isotropic attenuation power model, given by

$$S_i = \frac{S_0}{1 + \beta d_i^{\alpha}} \tag{13}$$

where S_0 is the signal strength of event source, β is a constant and d_i is the Euclidean distance between the node n_i and event source. The signal attenuation exponent is represented by α ranging from 2 to 3. For simplicity, we use $\beta = 1$ and $\alpha = 2$. Since we have used an average of sensed information by all the reporting nodes, the estimated value $\hat{S}_{\text{avg}}$ will be smaller than actual S. Let us assume that an event S triggers N reporting nodes within event radius R_{E} and $\hat{S}_{\text{avg}}$ will be an average of all the measured event information S_i from all these N nodes. Let this $\hat{S}_{\text{avg}}$ be equal to the decayed version of S at a distance of R_{c}, (where $R_{\text{c}} = R_{\text{E}}/\sqrt{2}$). Since we have used a simpler approach, $\hat{S}_i$, $\forall i$, is estimated using minimum mean square error (MMSE) at the sink. Using $\hat{S}_i$, $\hat{S}_{\text{avg}}$ is estimated, which is further scaled up to obtain $\hat{S}$ by a factor obtained from (13) for $d_i = R_{\text{c}}$. It should be noted that the estimation $\hat{S}_i$, $\forall i$, is also a JGRV with same properties, as the actual event information S_i, $\forall i$, is a JGRV. The sink will receive N measured values, as sample observations from N reporting nodes as given by

$$\boldsymbol{X} = \boldsymbol{A}\boldsymbol{Z} + \boldsymbol{W} \tag{14}$$

Here, the vector $\boldsymbol{X} \in \mathcal{R}^{N\times 1}$ is the sample observation, $\boldsymbol{Z} \in \mathcal{R}^{N\times 1}$ is the random vector for physically sensed event information, $\boldsymbol{A} \in \mathcal{R}^{N\times N}$ is the known transformation matrix and $\boldsymbol{W} \in \mathcal{R}^{N\times 1}$ represents noise vector. For simplicity, $\boldsymbol{A}$ is taken as identity matrix. Here, $\mathcal{R}$ is the set of real numbers. We also have

$$\begin{aligned} &\mathbb{E}[\boldsymbol{Z}] = \left[m_1,\ m_2,\ \ldots,\ m_N\right]^{\text{T}} \in \mathcal{R}^{N\times 1}, \\ &\mathbb{C}ov[\boldsymbol{Z}] = \boldsymbol{R}_{\boldsymbol{zz}} = \sigma_s^2 \boldsymbol{C}_{\boldsymbol{ss}} \in \mathcal{R}^{N\times N} \end{aligned} \tag{15}$$

where

$$\boldsymbol{C}_{\boldsymbol{ss}} = \begin{pmatrix} \rho_{(1,1)} & \rho_{(1,2)} & \cdots & \rho_{(1,N)} \\ \rho_{(2,1)} & \rho_{(2,2)} & \cdots & \rho_{(2,N)} \\ \vdots & \vdots & \ddots & \vdots \\ \rho_{(N,1)} & \rho_{(N,2)} & \cdots & \rho_{(N,N)} \end{pmatrix} \tag{16}$$

The elements of correlation matrix $\boldsymbol{C}_{\boldsymbol{ss}}$ is defined by our proposed correlation model (6). The MMSE estimate, $\hat{\boldsymbol{Z}}$ of $\boldsymbol{Z}$ can be formulated using the affine function [21] of $\boldsymbol{X}$ as

$$\hat{\boldsymbol{Z}} = \boldsymbol{K}\boldsymbol{X} + \boldsymbol{b} \tag{17}$$

where $\boldsymbol{K}$ is a matrix and $\boldsymbol{b}$ is a vector. It minimises the scalar MSE criterion. According to orthogonality principle [21], $\hat{\boldsymbol{Z}}$ will be a MMSE estimate if $\mathbb{E}\left[(\boldsymbol{Z} - \hat{\boldsymbol{Z}})\right] = 0$ and $\mathbb{E}\left[(\boldsymbol{Z} - \hat{\boldsymbol{Z}})\boldsymbol{X}^{\text{T}}\right] = 0$. Thus, we have

$$\boldsymbol{b} = \mathbb{E}[\boldsymbol{Z}] - \boldsymbol{K}\mathbb{E}[\boldsymbol{X}], \quad \boldsymbol{K} = \boldsymbol{R}_{\boldsymbol{zz}}\left(\boldsymbol{R}_{\boldsymbol{zz}} + \sigma_N^2 \boldsymbol{I}_N\right)^{-1} \tag{18}$$

Using (14), (15) and (18), (17) can be simplified as

$$\hat{\boldsymbol{Z}} = \mathbb{E}[\boldsymbol{Z}] + \boldsymbol{C}_{\boldsymbol{ss}}\left(\boldsymbol{C}_{\boldsymbol{ss}} + \frac{\sigma_N^2}{\sigma_S^2}\boldsymbol{I}_N\right)^{-1}\left(\boldsymbol{X} - \mathbb{E}[\boldsymbol{X}]\right) \tag{19}$$

The error covariance matrix, $\boldsymbol{R}_{\boldsymbol{ee}}$ can be calculated as

$$\begin{aligned} &\boldsymbol{R}_{\boldsymbol{ee}} = \mathbb{E}\left[(\boldsymbol{Z} - \hat{\boldsymbol{Z}})(\boldsymbol{Z} - \hat{\boldsymbol{Z}})^{\text{T}}\right] = \boldsymbol{R}_{\boldsymbol{zz}} - \boldsymbol{R}_{\boldsymbol{zz}}\left(\boldsymbol{R}_{\boldsymbol{zz}} + \sigma_N^2 \boldsymbol{I}_N\right)^{-1} \\ &\boldsymbol{R}_{\boldsymbol{zz}} = \left(\boldsymbol{R}_{\boldsymbol{zz}}^{-1} + \sigma_N^2 \boldsymbol{I}_N\right)^{-1} \end{aligned} \tag{20}$$

where second quantity is obtained using an identity $\boldsymbol{A}^{-1} + \boldsymbol{A}^{-1}\boldsymbol{C}(\boldsymbol{D} - \boldsymbol{B}\boldsymbol{A}^{-1}\boldsymbol{C})^{-1}\boldsymbol{B}\boldsymbol{A}^{-1} = (\boldsymbol{A} - \boldsymbol{C}\boldsymbol{D}^{-1}\boldsymbol{B})^{-1}$ [22].

Here, $\hat{\boldsymbol{Z}} = \left[\hat{S}_1,\ \hat{S}_2,\ \ldots,\ \hat{S}_N\right]^{\text{T}} \in \mathcal{R}^{N\times 1}$. The estimated values, $\hat{S}_i's$ are spatially correlated because the observed event information X_i's are spatially correlated. The too-much redundancy in data is not needed once the estimates are within distortion constraint (denoted by $D_{\max}$) as decided by application requirement. If somehow, only a subset of nodes is allowed to transmit, it will be good enough to meet this constraint $D_{\max}$. Therefore we investigate the achieved distortion when only M out of N nodes are selected to send event information to the sink. Since the estimator uses the average of estimate $\hat{S}_i$ with scaled version obtained from (13), $\hat{S}$, the estimate of S is given as

$$\begin{aligned} \hat{S}(M) &= \frac{\left(1 + R_{\text{c}}^2\right)}{M}\sum_{i=1}^{M}\hat{S}_i \\ &= \frac{\left(1 + R_{\text{c}}^2\right)}{M}[1,\ 1,\ \ldots,\ 1]\left[\hat{S}_1,\ \hat{S}_2,\ \ldots,\ \hat{S}_M\right]^{\text{T}} \end{aligned} \tag{21}$$

The event distortion achieved by selecting M packets, when each reporting node transmits only one report to the sink, can be estimated from average value of the sensed information. The achieved event distortion D_{E} is calculated as MSE [21, 22] that is equal to $\left(1 + R_{\text{c}}^2/M^2\right)\text{trace}(\boldsymbol{R}_{\boldsymbol{ee}})$ using (20) and (21). Here, trace($\boldsymbol{A}$) is the trace of the matrix $\boldsymbol{A}$. The calculation of distortion $D_{\text{E}}(N, M)$ can be simplified by selecting M nodes ($M < N$) through vector expansion in an alternative form as

$$D_{\text{E}}(N,\ M) = \mathbb{E}\left[\left(S(N) - \hat{S}(M)\right)^2\right] \tag{22}$$

doi: 10.1049/iet-wss.2012.0094

Expanding (22) using (11), (12) and (21)

$$D_{\mathrm{E}}(N,\ M) = \frac{\left(1+R_{\mathrm{c}}^2\right)^2}{\mathrm{NM}}\Bigg[N\sigma_s^2 + \sum_{i=1}^{N} m_i^2 + \sum_{i=1}^{M} m_i^2 - \frac{\sigma_s^4}{\left(\sigma_s^2+\sigma_N^2\right)}\left(2\sum_{i=1}^{N}\sum_{j=1 j\neq i}^{M}\rho_{(i,j)} - M\right) - 2\sum_{i=1}^{N}\sum_{j=1 j\neq i}^{M} m_i m_j + \sigma_s^2\sum_{i=1}^{N}\sum_{j=1 j\neq i}^{N}\rho_{(i,j)} + \frac{\sigma_s^6}{\left(\sigma_s^2+\sigma_N^2\right)^2}\sum_{i=1}^{M}\sum_{j=1 j\neq i}^{M}\rho_{(i,j)}\Bigg] \quad (23)$$

Here, the correlation coefficients $\rho_{(i,\ j)}$ are the elements of correlation matrix $\boldsymbol{C}_{\mathbf{ss}}$, which takes into account of sensing range and node separation. Using this distortion function, a case study has been presented in the next section.

5.2 Case studies for reconstruction performance

The achieved event distortion at the sink is computed using (23), which is the function of N reporting nodes, the correlation matrix $\boldsymbol{C}_{\mathbf{ss}}$ and R_{c}, whereas other parameters are constants such as M, m_i, σ_S and σ_N. In Section 5.2.1, we study the impacts of node density, selected node number and sensing range (where $r = \vartheta/2$) on the distortion performance using (23). As discussed in Section 3.3, the achieved distortion strongly depends on the correlation coefficient, $\rho_{(i,\ j)}$. In this case, the location of event source is not a necessary requirement. Unlike existing models [2, 3], our model does not need actual location of event source and thus will be more suitable for real network scenarios. A comparative study has also been provided in Section 5.2.2 to investigate the impacts of correlation coefficients on distortion performance. We extend the work of Vuran and Akyildiz [2] and Zheng and Tang [3] using an alternative event-driven sensing model and a new correlation function.

5.2.1 Case-1: impacts of node density and selected node number on distortion: In this subsection, the impacts of node density and the number of node selection on the reliability of event estimation at sink are studied. We conduct simulations over $\sqrt{N_{\mathrm{tot}}}d \times \sqrt{N_{\mathrm{tot}}}d\ m^2$ grid area, where N_{tot} sensor nodes are located on the grid. The node density is λ, as the number of nodes per unit area is $(1/d^2)$. We place an event source in the centre of grid area, where N nodes are activated within the event radius R_{E}. The simulations are performed with thousand trails and results are produced by averaging them as shown in Figs. 6 and 7. Fig. 6*a* shows results of the event distortion for different values of node density λ according to changing the number of selected nodes with respect to total reporting nodes (i.e. the ratio of total selected nodes to total reporting nodes) for a given event area. It is observed that the distortion approaches to relative by a constant value when the reporting nodes (i.e. M) are more than a threshold percentage of total nodes sensing the event (i.e. N). We have chosen the reporting nodes such that they should be as

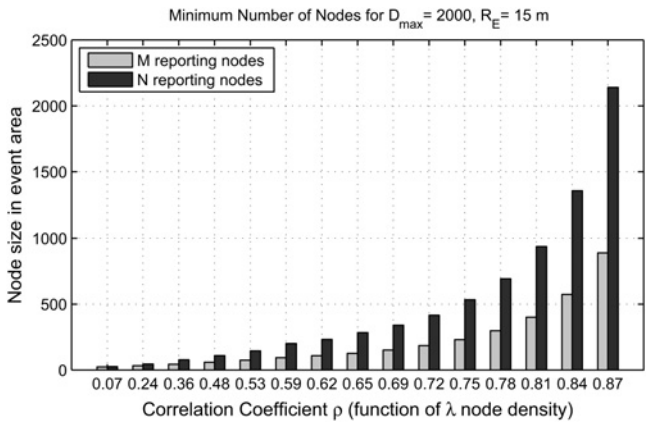

Fig. 7 *Optimal value of N_{min} reporting nodes with different correlation coefficients ρ*

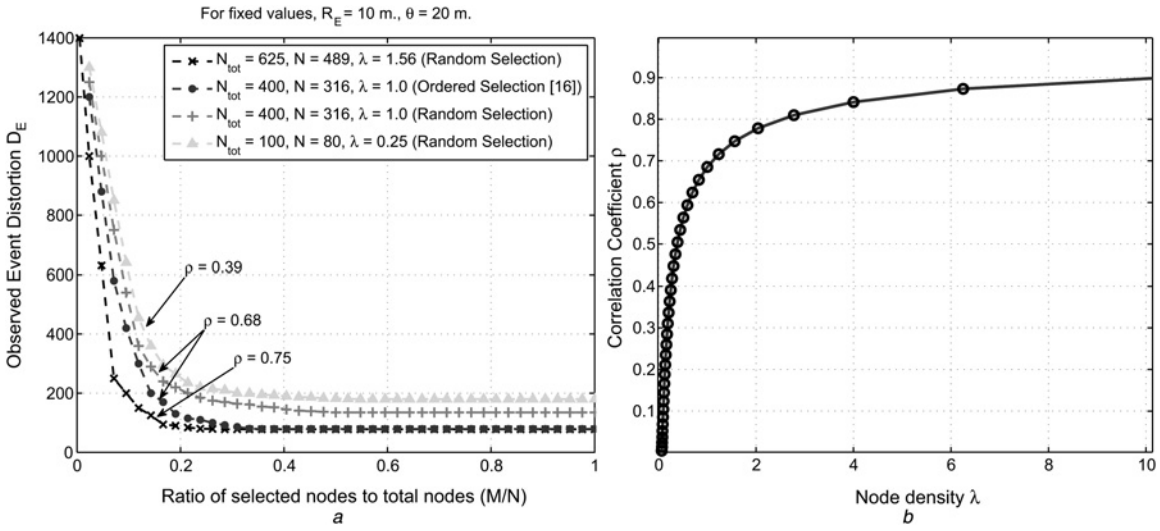

Fig. 6 *Average enent distortion as a function of the number of selected nodes for different p values*

a Average distortion for different λ values according to changing the number of selected nodes in the event area
b Change of correlation coefficient with node density λ for fixed θ = 4 m in the grid topology

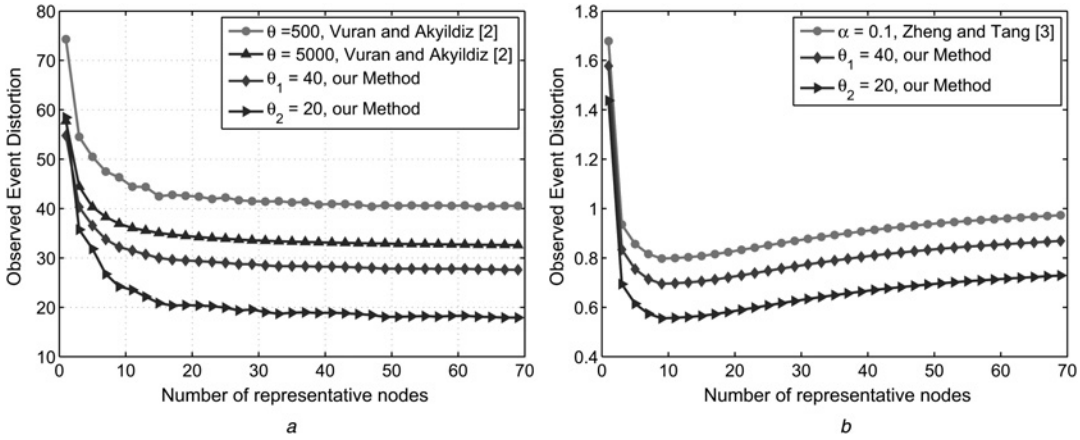

Fig. 8 *Comparison of average event distortion performance*

a Our method and the work of Vuran and Akyildiz [2]
b Our method and the work of Zheng and Tang [3]

close as possible to the centre of the area, where N nodes have sensed the information, whereas the reporting nodes are as far as possible from each other [18]. When node density λ increases, the spatial correlation coefficient also increases for fixed value of ϑ as shown in Fig. 6*b*. It means that a higher node density indicates a stronger correlation among data sample which results a better estimation reliability. Hence, the event distortion also becomes a monotonically decreasing function of λ as shown in Fig. 6*a*). On given 0.25 node density, 20% of total reporting nodes are sufficient to be activated for event reporting. This further implies that optimum performance can be achieved by allowing lesser number of reporting nodes M to be activated in the event area ($M < N$). Thus, the energy can be saved by exploiting spatial data correlation to limit the reporting nodes while ensuring acceptable distortion constraint $D_{\max}$. Fig. 7 shows results of the M reporting nodes for different values of correlation coefficient ρ when the observed event distortion does not exceed $D_{\max}$ at the sink.

5.2.2 Case-2 a comparative study: In the research work reported in [2, 3], a simple correlation model has been used for computing distortion in event reconstruction. Using this model, the expressions of distortion are derived to find the minimum number of representative nodes, M, out of total N nodes inside the event area. The minimum number M is needed to report data without exceeding the tolerable distortion constraint. Using the same expressions and assumptions as in [2, 3], we extend the work by applying our correlation model for the purpose of computing event distortion. In [2, 3], the power exponential model [19] is used as the correlation model to compute the event distortion. For same expressions of distortion, we use our proposed more realistic correlation model given by (6). To gain more insight into event reconstruction distortion using our correlation model, we conduct a comparative analysis with methods suggested in [2, 3], respectively. In a $1000 \times 1000\ \text{m}^2$ grid area, we have deployed 70 nodes randomly and a fixed event source in the centre of the grid area. The event reconstruction distortion has been calculated over a range of 0–70 sensor nodes that are sending event information to the sink. The simulation was performed using a fixed topology with thousand trials. The event distortion was evaluated using our and existing correlation models. These results are plotted in Fig. 8.

Fig. 8*a* shows a comparison of results obtained by methodology of Vuran and Akyildiz [2] using the power exponential model and our correlation model. For the given total N nodes, the distortion decreases logically with the increase in M representative nodes that are activated to send event information. This happens as more event information is received at the sink with larger M. However, using our model, at the same number of M representative nodes, even lesser distortion is achieved (see Table 3). It is shown that achieved distortion can be preserved at the sink using our model by allowing $N_{\min}$ nodes ($< M$) to be active. If somehow, only selected $N_{\min}$ nodes transmit event information, we can reduce the energy consumption. Fig. 8*b* shows a comparison using the method suggested in [3], between the earlier model and our model. It indicates the same behaviour that reduced achieved distortion allows a lower value of $N_{\min}$ which is less than M. Hence, using our correlation model, energy consumption in data transmissions and collisions can be minimised at the MAC layer.

Furthermore, the observed event distortion decreases with decreasing sensing range as shown in Figs. 6 and 8. To illustrate this, we can have a predefined $D_{\max}$ value as allowed by the sensor network application. The results obtained (Table 3) shows that for the minimum $D_{\max}$, θ_1 has to be 10 m, whereas for higher $D_{\max}$, θ_2 can be 111 m for same $N_{\min}$ (i.e. 15) representative nodes. Higher θ_2 implies that less number of nodes are used in the same field. Hence, for same $N_{\min}$ nodes and lesser distortion $D_{\max}$, the sensing range of nodes needs to be kept small through the control parameter (i.e. ϑ). Consequently, we can state, based on our correlation model, that the power consumption can be minimised by somehow allowing

Table 3 Results of ϑ for different values of $N_{\min}$ and $D_{\max}$

$N_{\min}$	$D_{\max}$					
	22	24	26	28	30	32
15	10	28	49	69	87	111
17	18	36	58	80	99	118
19	26	47	67	89	110	127
21	38	58	77	97	119	139
23	47	69	89	108	128	148
25	54	74	98	116	137	157

doi: 10.1049/iet-wss.2012.0094

smaller number of nodes to report the event while attaining the desired event reliability as specified by D_{max}. Both Figs. 8*a* and *b* indicate a lower bound on the minimum number of representative nodes that need to send the event information based on our correlation model.

6 Conclusions

In this paper, a basic correlation model has been introduced to represent the correlation characteristics between sensor nodes. Using the proposed correlation model, various key elements are discussed at both network and MAC layer. We found that the densely deployed WSN can be partitioned into non-overlapping correlated regions at the network layer. Thus, only single node needs to be allowed to report data rather than every node from a given correlated region, resulting in significant energy savings during data collection. Furthermore, our results show that required event reliability can be achieved through proper tuning of ϑ and ξ, that is, both the sensing range and the correlation threshold for reliable data delivery. In the context of MAC, we have investigated the impacts of node density, number of selected nodes and nodes' sensing range on the achieved event distortion at the sink. For the estimation of event source, the optimum node density within an event area can be found at the minimum observed event distortion. In addition, a comparative study showed that the proposed correlation model outperforms existing correlation models. We observed that optimal value of N_{min} nodes can be achieved through proper tuning of ϑ for given D_{max} as per application requirement. In this context, we also conclude that our approach takes into account the node location and sensing range. Most of the redundant transmissions can be filtered out on the basis of the presented model to make a more energy-efficient MAC design for sensor network applications.

7 References

1 Vuran, M.C., Akan, O.B., Akyildiz, I.F.: 'Spatio-temporal correlation: theory and applications for wireless sensor networks', *Comput. Netw. J. (Elsevier)*, 2004, **45**, pp. 245–259
2 Vuran, M.C., Akyildiz, I.F.: 'Spatial correlation based collaborative medium access control in wireless sensor networks', *IEEE/ACM Trans. Netw.*, 2006, **14**, (2), pp. 316–329
3 Zheng, G., Tang, S.: 'Spatial correlation-based MAC protocol for event-driven wireless sensor networks', *J. Netw.*, 2011, **6**, (1), pp. 121–128
4 Akyildiz, I.F., Vuran, M.C.: 'Wireless sensor networks' (John Wiley & Sons, 2010)
5 Scaglione, A., Servetto, S.: 'On the interdependence of routing and data compression in multi-hop sensor networks' (Wireless Networks (Elsevier), 2005), pp. 149–160
6 Yoon, S., Shahabi, C.: 'Exploiting spatial correlation towards an energy efficient clustered aggregation technique (CAG)'. Proc. ICC '05, Seoul, Korea, 2005, vol. 5, pp. 3307–3313
7 Pattem, S., Krishnmachari, B., Govindan, R.: 'The impact of spatial correlation on routing with compression in wireless sensor networks'. Proc. IPSN '04, Berkeley, California, USA, 2004, pp. 28–35
8 Pradhan, S.S., Kusuma, J., Ramchandran, K.: 'Distributed compression in a dense microsensor network', *IEEE Signal Proc. Mag.*, 2002, **19**, (2), pp. 51–60
9 Zahraie, M.S., Farkhady, A.Z., Haghighat, A.T.: 'Increasing network lifetime by optimum placement of sensors in wireless sensor networks'. Computer Modelling and Simulation, 2009. UKSIM'09. 11th Int. Conf., March 2009, pp. 611–616
10 Xiao, Y., Chen, H., Wu, K., *et al.*: 'Coverage and detection of a randomized scheduling algorithm in wireless sensor networks', *IEEE Trans. Comput.*, 2010, **59**, (4), pp. 507–521
11 Tezcan, N., Wang, W.: 'TTS: a two-tiered scheduling mechanism for energy conservation in wireless sensor networks', *Int. J. Sensor Netw.*, 2006, **1**, (3), pp. 213–228
12 Liu, C., Wu, K., Pei, J.: 'A dynamic clustering and scheduling approach to energy saving in data collection from wireless sensor networks'. Proc. Second IEEE Int. Conf. on Sensor and Ad Hoc Communications and Networks, September 2005
13 Dong, M., Tong, L., Sadler, B.: 'Impact of data retrieval pattern on homogeneous signal field reconstruction in dense sensor networks', *IEEE Trans. Signal Process.*, 2006, **54**, (11), pp. 4352–4364
14 Zhao, M., Chen, Z., Zhang, L., Ge, Z.: 'HS-Sift: hybrid spatial correlation-based medium access control for event-driven sensor networks', *IET Commun.*, 2007, **1**, (6), pp. 1126–1132
15 Guvensan, M.A., Yavuz, A.G.: 'On coverage issues in directional sensor networks: a survey', *Elsevier Ad Hoc Netw.*, 2011, **9**, (7), pp. 1238–1255
16 Ghosh, A., Das, S.K.: 'Coverage and connectivity issues in wireless sensor networks: a survey', *Pervasive Mob. Comput.*, 2008, **4**, (3), pp. 303–334
17 Shakya, R.K., Singh, Y.N., Verma, N.K.: 'A novel spatial correlation model for wireless sensor network applications'. Proc. Ninth IEEE Int. Conf. on Wireless and Optical communications Networks (WOCN'2012), September 2012, pp. 1–6
18 Shakya, R.K., Singh, Y.N., Verma, N.K.: 'A correlation model for MAC protocols in event-driven wireless sensor networks'. Proc. 2012 IEEE Region 10 Conf., (TENCON 2012), November 2012, pp. 1–6
19 Berger, J.O., de Oliviera, V., Sanso, B.: 'Objective bayesian analysis of spatially correlated data', *J. Am. Stat. Assoc.*, 2001, **96**, pp. 1361–1374
20 Garey, M.R., Johnson, D.S.: 'Computers and intractability; a guide to the theory of NP-completeness' (W.H. Freeman & Co., New York, NY, USA, 1990)
21 Kay, S.M.: 'Fundamentals of statistical signal processing vol. I: estimation theory' (Prentice-Hall, 1993)
22 Bhatia, R.: 'Matrix analysis' (Springer-Verlag, Graduate Texts in Mathematics, New York, 1991), Vol. 169

8 Appendix

8.1 Appendix 1

The flowchart of greedy correlated clustering algorithm is shown in Fig. 9.

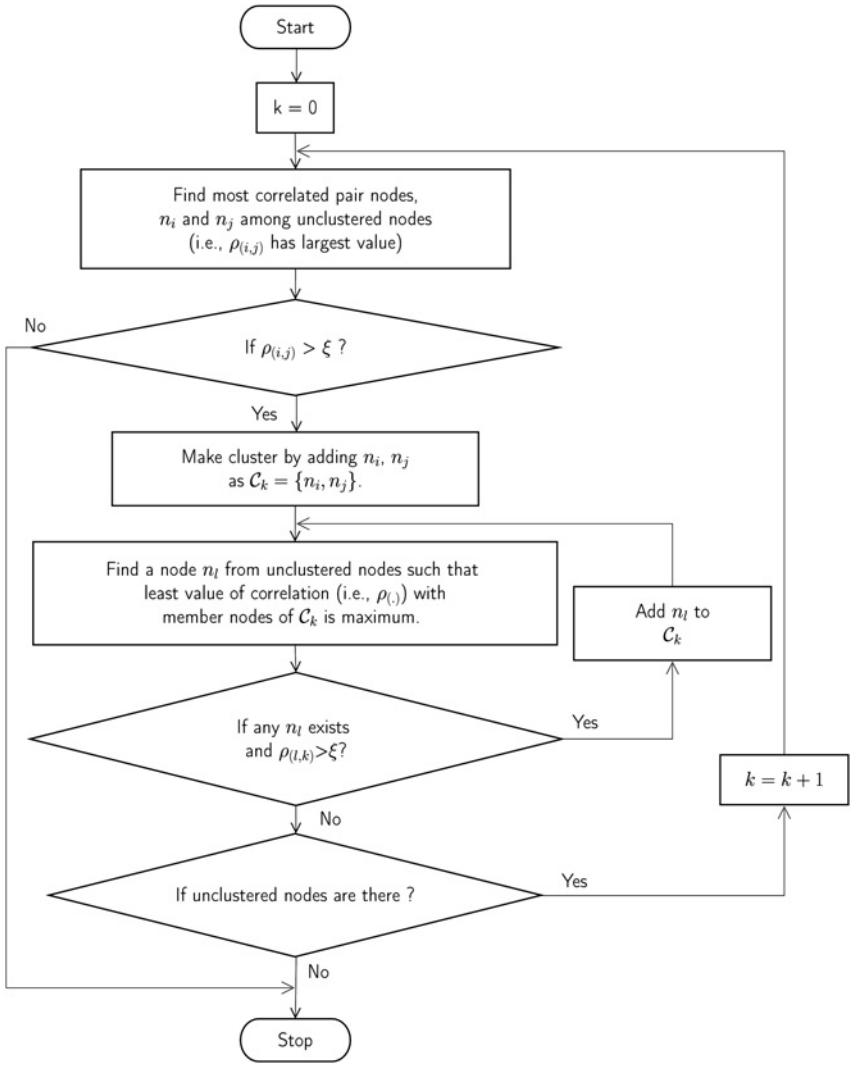

Fig. 9 *Flowchart of greedy correlated clustering algorithm*

doi: 10.1049/iet-wss.2012.0094